β-Arrestin2, interacting with phosphodiesterase 4, regulates synaptic release probability and presynaptic inhibition by opioids

Amyaouch Bradaïa*, Frédérique Berton*, Serge Ferrari†, and Christian Lüscher*‡§

*Department of Basic Neurosciences, ‡Clinic of Neurology, and †Department of Medicine and Service of Bone Diseases, University of Geneva, CH 1211 Geneva, Switzerland

Edited by Joseph A. Beavo, University of Washington School of Medicine, Seattle, WA, and approved January 12, 2005 (received for review September 8, 2004)

Most μ-opioid receptor agonists recruit β-arrestin2, with some exceptions such as morphine. Surprisingly, however, the acute analgesic effect of morphine is enhanced in the absence of β-arrestin2. To resolve this paradox, we examined the effects of morphine and fentanyl in acute brain slices of the locus coeruleus and the periaqueductal gray from β-arrestin2 knockout mice. We report that, in these mice, presynaptic inhibition of evoked inhibitory postsynaptic currents was enhanced, whereas postsynaptic G protein-coupled K^+ (Kir3/GIRK) currents were unaffected. The frequency, but not amplitude, of miniature inhibitory postsynaptic currents was increased in β-arrestin2 knockout mice, indicating a higher release probability compared to WT mice. The increased release probability resulted from increased cAMP levels because of impaired phosphodiesterase 4 function and conferred an enhanced efficacy of morphine to inhibit GABA release. Thus, β-arrestin2 attenuates presynaptic inhibition by opioids independent of μ-opioid receptor-driven recruitment, which may make β-arrestin2 a promising target for regulating analgesia.

synaptic transmission | μ-opioid receptors | locus coeruleus | periaqueductal gray | analgesia

Arrestin interaction with phosphorylated μ-opioid receptors (MORs) prompts desensitization of signaling by receptor uncoupling from G proteins followed by endocytosis (1). In addition, it has been found recently that during adrenergic signaling, β-arrestin2 forms a complex with phosphodiesterase 4 (PDE4). PDE4 is the cAMP-specific phosphodiesterase (2, 3); its interaction with β-arrestin2 thereby delivers the rate-limiting enzyme for cAMP degradation to the receptor site and thus quenches protein kinase A (PKA)-dependent processes (4–6).

In contrast to most other MOR agonists, morphine does not lead to β-arrestin recruitment and subsequent MOR internalization (7, 8). Nevertheless, opioid-mediated analgesia is strongly enhanced in β-arrestin2 knockout (KO) animals (9), but not in β-arrestin1 KO animals (8). The effects of morphine are mediated by two cellular functions localized in distinct compartments. Whereas activation of MORs expressed on the soma and dendrites leads to strong hyperpolarization of the neuron, MORs on synaptic terminals regulate transmitter release, in particular at GABAergic synapses (10). The molecular effectors have been shown to differ in the two cellular compartments. Postsynaptic inhibition is mediated by the activation of Kir3/GIRK channels (11, 12). Presynaptic inhibition, on the other hand, is caused by an inhibition of calcium channels (13), direct effects on the release machinery downstream of calcium entry (14), or activation of voltage-gated potassium channels (15).

Here, we have characterized the effects of the two MOR agonists, morphine and fentanyl, in acute slices of the locus coeruleus (LC) and the periaqueductal gray (PAG) of β-arrestin2 KO animals. The LC was chosen because it consists of a homogeneous population of adrenergic neurons that are ideal for studying pre- and postsynaptic inhibition because they postsynaptically express high levels of MORs and receive GABAergic afferents that are modulated by opioids (16). Moreover, activation of the central adrenergic system has been implicated to contribute to opioid analgesia (17). We also looked at the PAG, a central midbrain nucleus in the supraspinal pain-modulating circuit that is strongly disinhibited by opioids (18). In fact, the PAG consists of a heterogeneous population of neurons that have in common that they receive GABAergic afferents, which are inhibited by opioids (19).

We show that presynaptic inhibition by opioids is enhanced in β-arrestin2 KO mice and provide evidence that this effect results from an impaired activity of the cAMP-specific PDE4 (2, 3). Our data reveal that β-arrestin2 via the cAMP–PKA pathway thus determines the fundamental parameter of synaptic transmission, release probability (p_r), which is at the origin of the enhanced presynaptic inhibition.

Methods

Mice. All animal procedures were approved by the ethics committee on animal care and use at University of Geneva (Geneva) and carried out with the permission of the Cantonal Veterinary Office of Geneva. β-Arrestin2 KO mice were generated by F. Lin and R. Lefkowitz (Duke University Medical Center, Durham, NC) (9) and subsequently backcrossed for six generations onto a C57BL/6J background. The animals used in the present study were either WT and KO littermates resulting from heterozygous breeding or descendents of mice that were separately bred as homozygous WT or β-arrestin2 KO after the initial backcrossing. The genotype was verified by PCR of genomic DNA. Comparing data between β-arrestin2 KO animals (and between WT animals) in the two breeding colonies did not reveal any significant differences. As a consequence, differences between β-arrestin2 KO and the respective WT mice were of similar magnitude, and data were therefore pooled.

Electrophysiology in Acute Slice. Horizontal slices of the midbrain and the pons (250 μm thick, VT1000 vibratome, Leica) were prepared from postnatal day 15 (P15)–P25 mice brain by using standard procedures (20, 21) in cooled artificial cerebrospinal fluid containing 119 mM NaCl, 2.5 mM KCl, 1.3 mM $MgCl_2$, 2.5 mM $CaCl_2$, 1 mM NaH_2PO_4, 26.2 mM $NaHCO_3$, and 11 mM glucose, and continuously bubbled with 95% O_2 and 5% CO_2. Slices were progressively warmed up to 32–34°C, left to recover for at least 1 h, and then transferred to the recording chamber superfused (2 ml/min) with artificial cerebrospinal fluid. The visualized whole cell voltage-clamp recording technique was

This paper was submitted directly (Track II) to the PNAS office.

Abbreviations: MOR, μ-opioid receptor; PDE4, phosphodiesterase 4; LC, locus coeruleus; PAG, periaqueductal gray; KO, knockout; PSC, postsynaptic current; mIPSC, miniature inhibitory PSC; FSK, forksolin; eIPSC, evoked inhibitory PSC.

§To whom correspondence should be addressed. E-mail: christian.luscher@medecine.unige.ch.

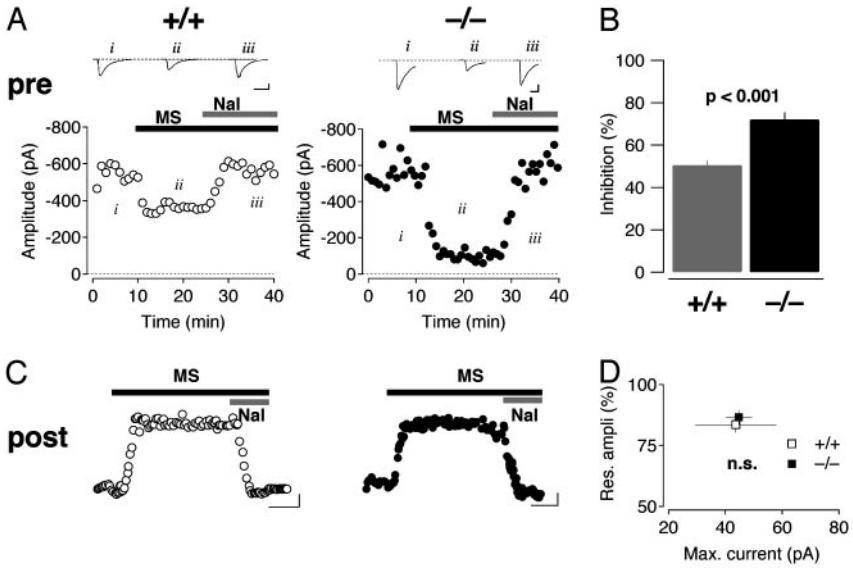

Fig. 1. Morphine-mediated pre- and postsynaptic inhibition in β-arrestin2 KO mice. (*A*) Morphine (MS, 10 μM) caused a decrease of the amplitude of GABAergic eIPSCs that was reversed by naloxone (NaI, 1 μM). The effect was more pronounced in β-arrestin2 KO (*Right*) compared with WT (*Left*) mice. Representative sweeps are averages of 20 individual traces. (Scale bars, 100 pA/20 ms.) (*B*) Bar graph reflecting eIPSC inhibition by morphine ($n = 6$ for each group, mean ± SEM). (*C*) Morphine (10 μM) applied for 15 min evoked a sustained outward current at a holding potential of −50 mV in WT and KO mice. (Scale bars, 10 pA/5 min.) (*D*) Normalized residual response after 10 min of morphine application as a function of the maximal current amplitude ($P > 0.05$, $n = 6$ for each genotype, mean ± SEM).

used to measure the holding current and synaptic responses of LC adrenergic neurons and neurons in the PAG. Synaptic currents were evoked by stimuli (0.1 ms) at 0.05 Hz through bipolar stainless steel electrodes positioned caudal to the LC or within the PAG in proximity (200–600 μm) of the recorded neuron. The internal solution contained 30 mM K-gluconate, 100 mM KCl, 4 mM $MgCl_2$, 10 mM creatine-phosphate, 3.4 mM Na_2ATP, 0.1 mM Na_3GTP, 1.1 mM EGTA, and 5 mM Hepes (pH adjusted to 7.3 with KOH). Currents were amplified (Multiclamp 700A, Axon Instruments, Foster City, CA), filtered at 1 kHz, digitized at 5 kHz (National Instruments Board PCI-MIO-16E4, NI-DAQ Igor Software, WaveMetrics, Lake Oswego, OR), and stored on hard disk. Cells were clamped at −50 mV, and elementary recordings consisted of sweeps of 3 s every 20 s for evoked responses and 30 s for miniature postsynaptic currents (PSCs). In each sweep, a 10-mV step was imposed to monitor cell membrane resistance and access resistance. The calculated reversal potential for Cl^- was $E_{Cl} = -4.7$ mV (Patcher's Power Tools, Max-Planck-Institut, Göttingen, Germany).

Compiled data are expressed as means ± SEM. Data were compared statistically either with Student's paired *t* test or the nonparametric Mann–Whitney test, and significance was assessed at $P < 0.05$ (INSTAT, version 3.0, GraphPad, San Diego). The detection and analysis of miniature synaptic currents were achieved by MINIANALYSIS software (version 6.0.4, Synaptosoft, Decatur, GA). The decay of miniature PSCs was analyzed from the peak of current to the return to the baseline current level with the least square algorithm provided by MINIANALYSIS. The evoked and miniature inhibitory PSC (mIPSC) decay phases were best fit by a single exponential function: $y = A \times \exp(-t/\tau)$ + baseline. Significant differences between two distributions of mIPSC amplitude and interevent intervals were determined by using the Kolmogorov–Smirnov test, with a *P* value <0.01 indicating significance.

cAMP Measurements. cAMP concentrations were measured with an ELISA kit (R & D Systems, DE0450) and normalized to the total protein content of the brain homogenate for comparison between samples from different animals.

Drugs. Naloxone, strychnine, forskolin (FSK), bicuculline, H8, 6-cyano-7-nitroquinoxaline-2,3-dione (CNQX), and kynurenic acid were obtained from Sigma. Tetrodotoxin was from Latoxan (Valence, France), morphine was from Amino (Neuenhof, Switzerland), and fentanyl was from Sintetica (Lugano, Switzerland). RO20–1724 [4-(3-butoxy-4-methoxyphenyl) methyl-2-imidazolidone] was obtained from Research Biochemicals International (Buchs, Switzerland).

Results

Pre- and Postsynaptic Inhibition of LC Neurons by Morphine. Morphine at 10 μM caused an inhibition of the evoked inhibitory PSC (eIPSC) that was stronger in β-arrestin2 KO mice than in WT animals (72.1 ± 3.4%, $n = 12$ vs. 50.5 ± 2.2%, $n = 10$, $P < 0.001$, Fig. 1 *A* and *B*). Further quantification of presynaptic inhibition by morphine confirmed that the absence of β-arrestin2 resulted in higher efficacy for morphine (see Fig. 7*C Left*). Similarly, the high-affinity agonist fentanyl also inhibited eIPSC in the LC with greater efficacy in β-arrestin2 KO animals compared to WT controls (see Fig. 7*C Right*).

MOR-evoked PSCs in the LC are carried almost exclusively by Kir/GIRK channels (11, 22). In accordance with previous reports, we elicited sustained outward currents with morphine in WT animals (20, 23, 24). Moreover, the maximum amplitude and the weak desensitization were undistinguishable from the responses obtained in β-arrestin2 mice ($n = 6$ for each genotype; $P > 0.05$, Fig. 1 *C* and *D*).

Taken together, the absence of β-arrestin2 led to enhanced presynaptic inhibition but did not change the maximal amplitude nor the degree of desensitization of morphine currents. To elucidate the mechanism underlying this dissociation, we further characterized GABAergic transmission in β-arrestin2 KO mice.

Increased mIPSC Frequency and Decreased Paired Pulse Ratio of eIPSCs. GABAergic transmission was pharmacologically isolated with the glutamate receptors and glycine receptor antagonists

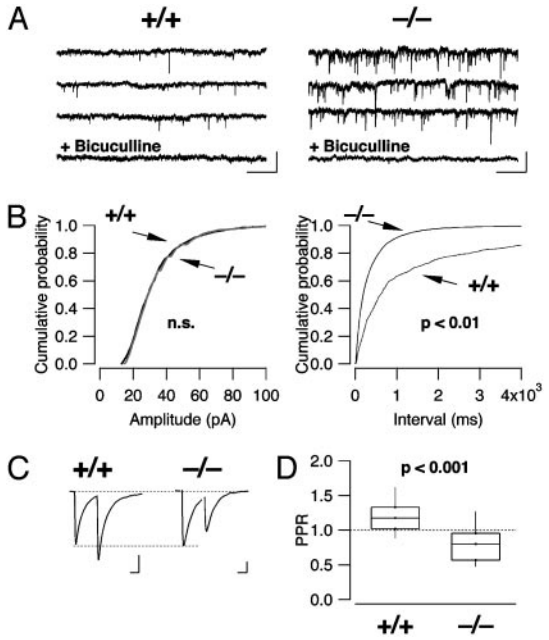

Fig. 2. Characterization of GABAergic mIPSCs and paired pulse ratio of eIPSCs. (*A*) Examples of mIPSCs recorded in WT (*Left*) and KO mice (*Right*). (Scale bars, 50 pA/2 s.) (*B*) Cumulative probability histograms of amplitudes and interevent intervals of mIPSCs in the WT (gray trace, $n = 15$) and KO mice (black, $n = 18$). In the KO mice, the distribution of the interevent intervals is significantly shifted to the left, indicating an increase in mIPSC frequency. (*C*) A paired pulse stimulation (0.1-ms duration, 50-ms interval) elicited eIPSCs in WT mice that show paired pulse facilitation in WT mice (*Left*, average of 20 sweeps), whereas paired pulse depression was observed in KO mice (*Right*). (Scale bars, 200 pA per 20 ms for WT mice, 100 pA per 20 ms for KO mice.) (*D*) Box plot of the paired pulse ratio in the WT and KO mice, indicating 10th, 25th, 50th, 75th, and 90th percentile ($P < 0.001$, $n = 34$ and 31, respectively).

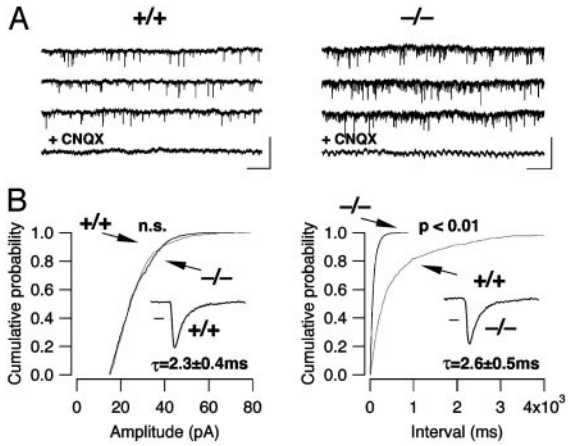

Fig. 3. Characterization of glutamatergic mEPSCs. (*A*) Examples of mEPSCs recorded in WT (*Left*) and KO (*Right*) mice at −50 mV in the presence of tetrodotoxin (0.5 μM), bicuculline (10 μM), and strychnine (1 μM). (Scale bars, 100 pA/2 s.) mEPSCs were sensitive to 6-cyano-7-nitroquinoxaline-2,3-dione (CNQX) (10 μM), which in the cell of the KO mouse revealed an oscillatory membrane potential characteristic of LC neurons. (*B*) Cumulative probability histograms of amplitudes and interevent intervals of mEPSCs in the WT (gray trace, $n = 4$) and KO mice (black trace, $n = 4$). In the KO mice, the distribution of the interevent intervals is significantly shifted to the left (Kolmogorov–Smirnov test, $P < 0.01$), indicating an increase in mEPSC frequency. (*Insets*) The decay of an average mEPSC (100 scaled and averaged events) was fitted with a monoexponential function; no significant difference was found. (Scale bar, 2 ms, $P > 0.05$.)

kynurenic acid (2 mM) and strychnine (1 μM). In addition, action potentials were blocked with tetrodotoxin (0.5 μM), and inward mIPSCs were then collected for 10–15 min with the cell voltage clamped at 45 mV below E_{Cl}. The events collected under these conditions had a mean frequency of 0.48 ± 0.7 Hz in WT animals ($n = 24$) and 2.9 ± 0.5 Hz in β-arrestin2 KO mice ($n = 29$, $P < 0.01$) and were sensitive to bicuculline (Fig. 2*A*). In contrast, neither the mean mIPSC amplitude (24.7 ± 1.4 pA for the WT mice and 25.9 ± 0.9 pA for the KO mice, $P > 0.05$, $n = 12$, Fig. 2*B Left*) nor the decay kinetics (28.9 ± 1.5 ms vs. 29.2 ± 1.7 ms, $n = 12$ each group, not shown) differed between WT and KO mice. This isolated increase of the frequency of mIPSCs suggests that the presynaptic p_r for GABA was significantly higher in β-arrestin2 KO mice compared with WT controls. A similar increase of the frequency of spontaneous events was also observed for miniature excitatory synaptic currents (mEPSCs, Fig. 3). Because MORs are mainly expressed on inhibitory afferents to the LC (10), we focused on GABAergic transmission in the subsequent experiments.

To test whether evoked GABA release was also affected by this change of p_r, we applied a paired-pulse stimulation to the slice to determine the paired pulse ratio of eIPSCs. It is well established that, in low p_r synapses, the second release will be strongly enhanced because of residual calcium in the presynaptic terminal. This facilitation is smaller in high p_r synapses and may even reveal a depression of the synaptic current evoked by the second stimulus. Changes in paired pulse ratio have therefore become a standard tool to estimate changes in p_r (25). We observed paired-pulse facilitation in WT mice (paired pulse ratio = 1.28 ± 0.09, $n = 34$), and paired-pulse depression in β-arrestin2 KO animals (paired pulse ratio = 0.80 ± 0.05, $n = 31$, $P < 0.001$, Fig. 2 *C* and *D*). Again, no change of the decay time of the eIPSC was observed between the two genotypes (data not shown).

Similarly, recordings performed in the PAG also revealed a significantly higher frequency of mIPSCs in β-arrestin2 KO mice without any difference in their amplitude (0.33 ± 0.16 Hz in WT mice vs. 3.26 ± 0.56 Hz in β-arrestin2 KO mice, $P < 0.01$; amplitude: 27.4 ± 2.7 pA WT, 24.5 ± 1.7 pA KO, $P > 0.05$, $n = 6$ for each genotype, Fig. 4 *A* and *B*). In accordance with previous reports (26), evoked IPSCs were sensitive to opioid agonists. As described above for morphine in the LC, we found that fentanyl at 100 nM caused a much stronger inhibition in KO animals compared to WT (63 ± 1.4% vs. 28.3 ± 2.0%, $P < 0.01$, $n = 5$ for each genotype, Fig. 4 *C* and *D*).

Taken together, the observations of mIPSCs in the LC and PAG and eIPSCs in LC indicate that p_r for spontaneous and evoked release of GABA was significantly higher in the KO mice compared to WT controls, and was associated with enhanced presynaptic inhibition to opioids.

Involvement of the cAMP–PKA Pathway. To examine a possible involvement of the cAMP–PKA pathway in the increased p_r in LC of KO mice, we pharmacologically activated adenylyl cyclase by bath-applying FSK. FSK (5 μM) significantly increased the frequency of mIPSC in the WT mice (from 0.6 ± 0.1 Hz in control condition to 2.8 ± 0.3 Hz in the presence of FSK, $P < 0.01$, $n = 5$) but had no effect on the frequency of mIPSCs in the KO mice (2.3 ± 0.4 Hz in control condition vs. 2.3 ± 0.3 Hz with FSK, $n = 5$, Fig. 5 *A* and *B*). As expected, FSK did not change the amplitude of the mIPSC in neither WT nor KO mice (data not shown).

Because β-arrestin2 may form a complex with PDE4, the increased cAMP concentrations in presynaptic terminals of KO mice could be the result of a decrease in cAMP degradation (4–6). To test this, we selectively inhibited PDE4 by bath applying 4-[(3-butoxy-4-methoxyphenyl)-methyl]-2-imidazolidi-

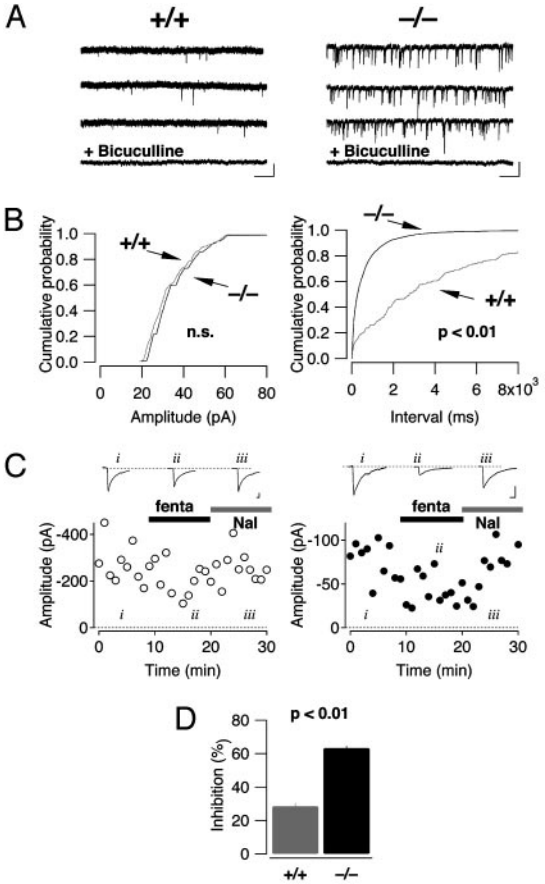

Fig. 4. Increased mIPSC frequency and enhanced presynaptic inhibition by fentanyl in neurons of the PAG. (*A*) Examples of mIPSCs recorded in WT (*Left*) and KO (*Right*) mice at −50 mV in the presence of tetrodotoxin (0.5 μM), kynurenic acid (2 mM), and strychnine (1 μM). (Scale bars, 50 pA/2 s.) mTPSCs were sensitive to bicuculline. (*B*) Cumulative probability histograms of amplitudes and interevent intervals of mIPSCs in the WT (gray trace, $n = 6$) and KO (black trace, $n = 6$) mice. In the KO mice, the distribution of the interevent intervals is significantly shifted to the left (Kolmogorov–Smirnov test, $P < 0.01$), indicating an increase in mIPSC frequency. (*C*) Fentanyl (fenta, 100 nM) caused a decrease of the amplitude of GABAergic eIPSCs that was reversed by naloxone (Nal, 1 μM). The effect was more pronounced in β-arrestin2 KO (*Right*) compared with WT (*Left*) mice. Representative sweeps are averages of 20 individual traces. (Scale bars, 50 pA/20 ms.) (*D*) Bar graph reflecting eIPSC inhibition by fentanyl ($n = 5$ for each group, mean ± SEM).

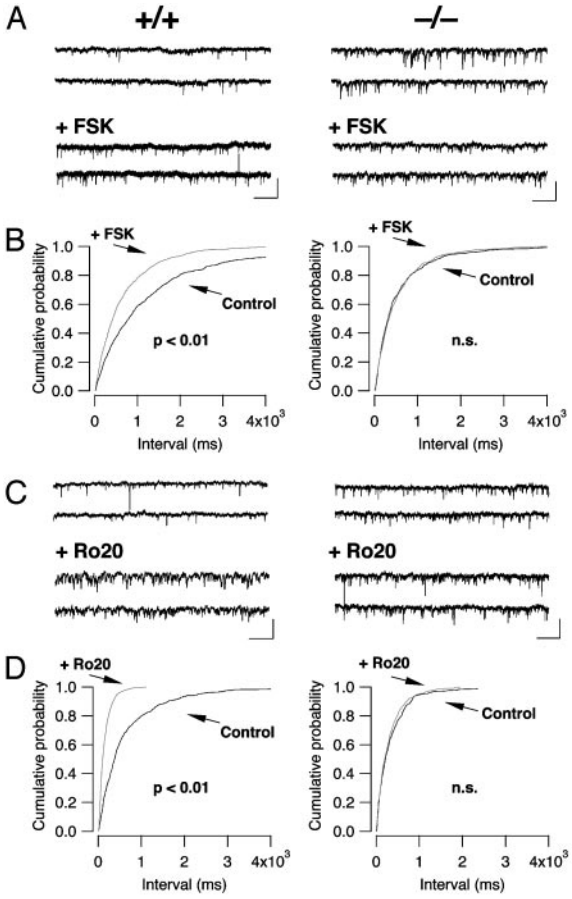

Fig. 5. FSK and Ro-20–1724 increase the mIPSC frequency in the WT mice but not in the KO mice. (*A*) Representative traces before [top two traces, from WT (*Left*) or KO (*Right*) mice] and after (bottom two traces) 5 μM FSK application. (*B*) FSK induced a shift in the cumulative probability histogram of interevent intervals in WT (*Left*) that was occluded by the higher basal mIPSC frequency in KO (*Right*) animals. (*C* and *D*) The increase of the mIPSC frequency observed in WT mice with the PDE inhibitor, Ro-20-1724, was occluded in KO mice. (Scale bars, 50 pA/2 s.)

none (Ro-20-1724) (27). Ro-20-1724 (50 μM) significantly increased the frequency of mIPSC in WT mice (0.5 ± 0.1 Hz in control condition and 2.5 ± 0.2 Hz in the presence of Ro-20-1724, $n = 4$) but had no effect on the frequency of the mIPSC in the KO mice (2.9 ± 0.5 Hz in control condition and 2.8 ± 0.6 Hz in the presence of Ro-20-1724, $n = 4$, Fig. 5 *C* and *D*). A similar occlusion of the frequency increase by Ro-20-1724 was also observed for glutamatergic mEPSCs (data not shown).

To evaluate whether any cAMP levels were generally increased in the brain of KO mice or whether changes were restricted to the presynaptic terminals, we measured the absolute value of cAMP in homogenates of the cortex and the midbrain of both genotypes. The unstimulated cAMP levels observed were lower in the midbrain compared to the cortex, but similar in WT and KO animals. This finding rules out a general increase but does not preclude increases in very restricted compartments such as the presynaptic terminals (Fig. 6, $n = 3$ for each condition).

If the cAMP–PKA pathway mediates the increase in p_r seen in β-arrestin2 KO mice, then a PKA inhibitor should have a bigger effect in β-arrestin2 KO mice than in WT. Consistent with this prediction, H8 (10 μM) had no effect in WT mice but reduced mIPSC frequency to control levels in β-arrestin2 KO mice (from 2.5 ± 0.8 Hz in control condition to 0.6 ± 0.1 Hz in the presence of H8, $P < 0.01$, $n = 4$, Fig. 7 *A* and *B*). H8 had no effect on the mIPSC amplitude (data not shown).

Taken together, these results indicate that the enhanced p_r in β-arrestin2 KO mice is mediated by impaired constitutive, MOR-independent recruitment of PDE4 activity and a subsequent increase of cAMP at presynaptic release sites.

Finally, we examined whether the increased levels of cAMP were also responsible for the enhanced efficacy of morphine for presynaptic inhibition. In slices of β-arrestin2 KO animals, H8 reversed the enhanced efficacy of morphine. In fact, quantifying presynaptic inhibition at increasing concentrations of morphine in KO mice showed that the dose–response curve after H8 treatment was superimposable to WT controls (Fig. 7*C Left*). Finally, to directly compare the effects of the two MOR agonists morphine and fentanyl on the same synapse, we determined the concentration–response curves for presynaptic inhibition in the LC and revealed again a shift to the left in KO animals, but without a significant enhancement of the maximal effect.

Discussion

p_r is a basic property of a given synaptic terminal that crucially determines its function. This probability can be regulated in

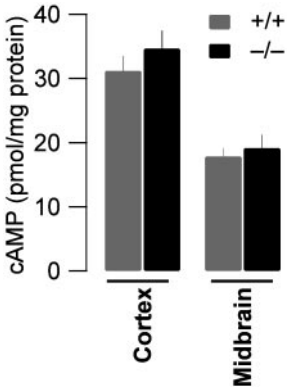

Fig. 6. Similar overall cAMP concentration between genotypes. Measuring the total concentration of cAMP normalized to the total protein content of homogenates obtained from cortex (31.2 ± 2.3 vs. 34.7 ± 2.8 pmol/mg) and midbrain (17.9 ± 1.3 vs. 19.2 ± 2.1 pmol/mg) of WT and β-arrestin2 KO mice did not show any significant difference between the genotypes ($P < 0.05$, $n = 3$).

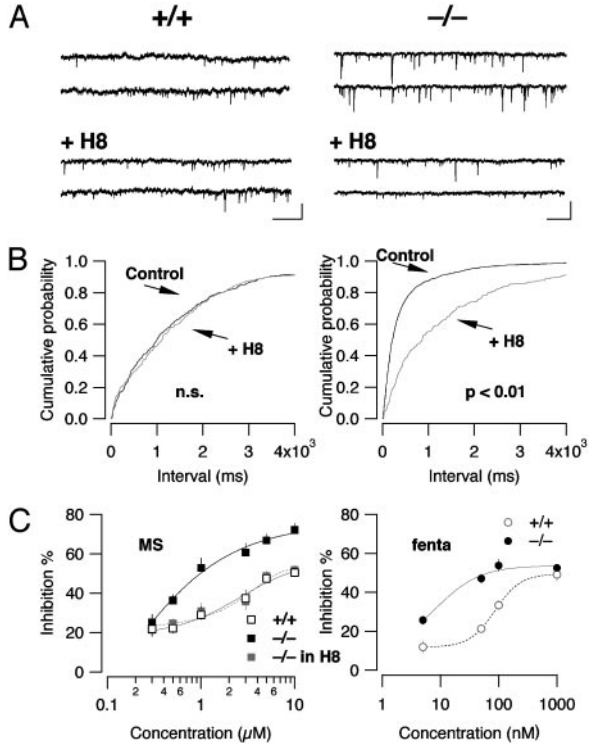

Fig. 7. The PKA inhibitor H8 lowers mIPSC frequency and reverses enhanced presynaptic inhibition in β-arrestin2 KO mice. (*A*) Representative traces before [top two traces, from WT (*Left*) or from KO (*Right*) mice] and after 20 min of application of H8 (5 μM, bottom two traces). (*B*) H8 induced a shift to the right in the cumulative probability histogram of interevent intervals in KO (*Right*) but not in WT (*Left*) animals. (Scale bars, 50 pA/2 s.) (*C*) Dose–response curves for presynaptic inhibition of eIPSCs by morphine (MS) in WT (open symbols), KO (black symbols, $P < 0.01$ compared with WT for all concentrations >1 μM), and KO in the presence of H8 (gray symbol). Note that the curves fitted with the Hill equation were indistinguishable for WT and KO treated with H8 ($n = 5$, mean ± SEM). (*Right*) concentration–response curve for presynaptic inhibition of eIPSC in LC by fentanyl (fenta).

association with many forms of synaptic plasticity and is a function of the level of cAMP in the terminal. Increased cAMP concentration enhances p_r either through PKA activity (28, 29), regulating the size of the releasable vesicle pool (30), or other signaling pathways, such as the Epac pathway (31). Our observation that the PKA inhibitor H8 reverses the high mIPSCs frequency and the enhanced efficacy of morphine suggests a constitutive PKA-dependent process. PDE4 is translocated to the membrane along with β-arrestin2 after adrenergic receptor activation, but there is evidence that the β-arrestin2–PDE4 complexes are present in the cytosol (4). Our finding that p_r is higher in the absence of β-arrestin2 may reflect a constitutive activation of PDE4 bound to cytoplasmic β-arrestin2. Alternatively, constitutively active G protein-coupled receptors (or receptors activated by ambient agonists) could recruit the β-arrestin2–PDE4 complex to the release sites and lower basal p_r. Given that PDE4 enzymes are inherently active (32) and that we did not detect general increase of cAMP concentration in brain homogenates, the latter scenario seems more likely.

Normally, G_{io}-coupled receptors cause presynaptic inhibition independent of adenylyl cyclase inhibition (13). This may change in situations where cAMP concentrations are high. Under these circumstances, G_{io}-mediated reduction of cAMP may have an effect on release that adds to the basic inhibition. In fact, a cAMP-dependent component of presynaptic inhibition that directly modulates vesicle priming has recently been described (33). Moreover, when cAMP levels increase during withdrawal after chronic exposure to morphine, the p_r of GABAergic synapses increases, leading to stronger presynaptic inhibition by morphine (34, 35). A similar mechanism appears to operate in β-arrestin2 KO mice, which may explain the enhanced efficacy to opioids and its reversal by PKA inhibitors.

At the systemic level, the concomitant increase in p_r of both GABAergic and glutamatergic transmission may explain the absence of a more pronounced phenotype in KO mice, such as epileptic seizures or strong alterations of basal nociception. However, our data raise the possibility that an enhanced presynaptic effect may underlie the enhanced morphine analgesia observed in β-arrestin2 KO mice. This finding implies that, in WT animals, presynaptic inhibition of GABA release in supraspinal nuclei significantly contributes to opioid analgesia. In the PAG, for example, strong GABAergic afferents that are part of the descending antinociceptive pathway are important targets of opioids in the central nervous system (18). Inhibiting transmitter release at this synapse may mediate analgesic effects of opioids. The importance of presynaptic inhibition is apparent from the finding that, in the absence of GIRK2, morphine still very efficiently increases latencies in a nociceptive test (36). Finally, there is also evidence that disinhibition of adrenergic neurons of the LC contributes to supraspinal analgesia by morphine (10). In this study, evidence is provided that a subset of LC neurons can effectively be activated through presynaptic inhibition of GABAergic afferents.

In vivo, analgesia is enhanced in β-arrestin2 KO animals in response to morphine and heroin but not in response to agonists that readily trigger MOR endocytosis such as fentanyl (37). At first, this seems contradictory to our observation that the presynaptic inhibition by fentanyl is enhanced in β-arrestin2 KO mice. However, the maximal presynaptic inhibition caused by a saturating concentration of fentanyl was not significantly different from WT animals, which may explain the absence of an enhancement in the behavioral test.

In conclusion, we have provided evidence that β-arrestin2 through an interaction with PDE4 determines the fundamental parameter of synaptic transmission p_r and confers enhanced presynaptic inhibition. This mechanism may regulate the analgesic efficacy of opioids without direct recruitment of β-arrestin2 by MORs. Our findings support early data in rodents (38), as well as more recent findings including studies on PDE4 KO mice (39), and human clinical trials indicating that centrally active PDE4

inhibitors (40) could, in fact, be used to enhance the analgesic effects of opioids.

We thank the members of the C.L. laboratory for many helpful discussions; R. Lefkowitz for support and providing the KO animals; M. Serafin, M. Frerking, D. Muller, and P. Slesinger for comments on an earlier version of the manuscript; and F. Loctin, D. Manen, and D. Pierroz for technical assistance. C.L. is supported by grants from the Swiss National Science Foundation and the de Reuter and Schmidheiny Foundations and by a Human Science Frontier Program Young Investigator grant. S.F. is supported by grants of the Swiss National Science Foundation, the Roche Research Foundation, and the Swiss Foundation for Aging Research.

1. Gainetdinov, R. R., Premont, R. T., Bohn, L. M., Lefkowitz, R. J. & Caron, M. G. (2004) *Annu. Rev. Neurosci.* **27,** 107–144.
2. Conti, M., Richter, W., Mehats, C., Livera, G., Park, J. Y. & Jin, C. (2003) *J. Biol. Chem.* **278,** 5493–5496.
3. Houslay, M. D. & Adams, D. R. (2003) *Biochem. J.* **370,** 1–18.
4. Perry, S. J., Baillie, G. S., Kohout, T. A., McPhee, I., Magiera, M. M., Ang, K. L., Miller, W. E., McLean, A. J., Conti, M., Houslay, M. D. & Lefkowitz, R. J. (2002) *Science* **298,** 834–836.
5. Baillie, G. S., Sood, A., McPhee, I., Gall, I., Perry, S. J., Lefkowitz, R. J. & Houslay, M. D. (2003) *Proc. Natl. Acad. Sci. USA* **100,** 940–945.
6. Bolger, G. B., McCahill, A., Huston, E., Cheung, Y. F., McSorley, T., Baillie, G. S. & Houslay, M. D. (2003) *J. Biol. Chem.* **278,** 49230–49238.
7. Whistler, J. L. & von Zastrow, M. (1998) *Proc. Natl. Acad. Sci. USA* **95,** 9914–9919.
8. Bohn, L. M., Dykstra, L. A., Lefkowitz, R. J., Caron, M. G. & Barak, L. S. (2004) *Mol. Pharmacol.* **66,** 106–112.
9. Bohn, L. M., Lefkowitz, R. J., Gainetdinov, R. R., Peppel, K., Caron, M. G. & Lin, F. T. (1999) *Science* **286,** 2495–2498.
10. Pan, Y. Z., Li, D. P., Chen, S. R. & Pan, H. L. (2004) *Brain Res.* **997,** 67–78.
11. Torrecilla, M., Marker, C. L., Cintora, S. C., Stoffel, M., Williams, J. T. & Wickman, K. (2002) *J. Neurosci.* **22,** 4328–4334.
12. Lüscher, C., Jan, L. Y., Stoffel, M., Malenka, R. C. & Nicoll, R. A. (1997) *Neuron* **19,** 687–695.
13. Miller, R. J. (1998) *Annu. Rev. Pharmacol. Toxicol.* **38,** 201–227.
14. Scanziani, M., Capogna, M., Gahwiler, B. H. & Thompson, S. M. (1992) *Neuron* **9,** 919–927.
15. Vaughan, C. W., Ingram, S. L., Connor, M. A. & Christie, M. J. (1997) *Nature* **390,** 611–614.
16. Cohen, G. A., Doze, V. A. & Madison, D. V. (1992) *Neuron* **9,** 325–335.
17. Jones, S. L. & Gebhart, G. F. (1986) *J. Neurophysiol.* **56,** 1397–1410.
18. Fields, H. (2004) *Nat. Rev. Neurosci.* **5,** 565–575.
19. Osborne, P. B., Vaughan, C. W., Wilson, H. I. & Christie, M. J. (1996) *J. Physiol.* **490,** 383–389.
20. Blanchet, C. & Lüscher, C. (2002) *Proc. Natl. Acad. Sci. USA* **99,** 4674–4679.
21. Blanchet, C., Sollini, M. & Luscher, C. (2003) *Mol. Cell. Neurosci.* **24,** 517–523.
22. Cruz, H. G., Ivanova, T., Lunn, M. L., Stoffel, M., Slesinger, P. A. & Lüscher, C. (2004) *Nat. Neurosci.* **7,** 153–159.
23. Osborne, P. B. & Williams, J. T. (1995) *Br. J. Pharmacol.* **115,** 925–932.
24. Bailey, C. P., Couch, D., Johnson, E., Griffiths, K., Kelly, E. & Henderson, G. (2003) *J. Neurosci.* **23,** 10515–10520.
25. Stuart, G. J. & Redman, S. J. (1991) *Neurosci. Lett.* **126,** 179–183.
26. Vaughan, C. W. & Christie, M. J. (1997) *J. Physiol. (London)* **498,** 463–472.
27. Reeves, M. L., Leigh, B. K. & England, P. J. (1987) *Biochem. J.* **241,** 535–541.
28. Chavez-Noriega, L. E. & Stevens, C. F. (1994) *J. Neurosci.* **14,** 310–317.
29. Weisskopf, M. G., Castillo, P. E., Zalutsky, R. A. & Nicoll, R. A. (1994) *Science* **265,** 1878–1882.
30. Nagy, G., Reim, K., Matti, U., Brose, N., Binz, T., Rettig, J., Neher, E. & Sorensen, J. B. (2004) *Neuron* **41,** 417–429.
31. Kaneko, M. & Takahashi, T. (2004) *J. Neurosci.* **24,** 5202–5208.
32. Beavo, J. A. & Brunton, L. L. (2002) *Nat. Rev. Mol. Cell. Biol.* **3,** 710–718.
33. Sakaba, T. & Neher, E. (2003) *Nature* **424,** 775–778.
34. Hack, S. P., Vaughan, C. W. & Christie, M. J. (2003) *Neuropharmacology* **45,** 575–584.
35. Ingram, S. L., Vaughan, C. W., Bagley, E. E., Connor, M. & Christie, M. J. (1998) *J. Neurosci.* **18,** 10269–10276.
36. Mitrovic, I., Margeta-Mitrovic, M., Bader, S., Stoffel, M., Jan, L. Y. & Basbaum, A. I. (2003) *Proc. Natl. Acad. Sci. USA* **100,** 271–276.
37. Minnis, J. G., Patierno, S., Kohlmeier, S. E., Brecha, N. C., Tonini, M. & Sternini, C. (2003) *Neuroscience* **119,** 33–42.
38. Nicholson, D., Reid, A. & Sawynok, J. (1991) *Pharmacol. Biochem. Behav.* **38,** 753–758.
39. Robichaud, A., Stamatiou, P. B., Jin, S. L., Lachance, N., MacDonald, D., Laliberte, F., Liu, S., Huang, Z., Conti, M. & Chan, C. C. (2002) *J. Clin. Invest.* **110,** 1045–1052.
40. O'Donnell, J. M. & Zhang, H. T. (2004) *Trends Pharmacol. Sci.* **25,** 158–163.